Parity-time symmetry under magnetic flux

L. Jin[*] and Z. Song

School of Physics, Nankai University, Tianjin 300071, China
(Received 4 December 2015; published 8 June 2016)

We study a parity-time–($\mathcal{PT}$-) symmetric ring lattice, with one pair of balanced gain and loss located at opposite positions. The system remains $\mathcal{PT}$-symmetric when threaded by a magnetic flux; however, the $\mathcal{PT}$ symmetry is sensitive to the magnetic flux in the presence of a large balanced gain and loss, or in a large system. We find a threshold gain or loss above which any nontrivial magnetic flux breaks the $\mathcal{PT}$ symmetry. We obtain the maximally tolerable magnetic flux for the exact $\mathcal{PT}$-symmetric phase, which is approximately linearly dependent on a weak gain or loss.

I. INTRODUCTION

A magnetic flux enclosed in electron trajectories induces electron wave-function interference; this is the well-known magnetic Aharonov-Bohm (AB) effect [1,2]. The AB effect describes a quantum phenomenon in which a charged particle is affected by the vector potential of an electromagnetic field. The AB effect has inspired breakthroughs in modern physics. Photons are known to be neutral particles that do not directly interact with magnetic fields. However, the magnetic AB effect for photons has been proposed and realized by magnetic-optical effects [3], dynamical modulation [4], and photon-phonon interaction [5]. This is attributed to an effective magnetic field originating from the fictitious gauge field felt by photons, where photons behave as electrons in a magnetic field. The concept of an effective magnetic field for photons provides new opportunities in optics; it stimulates interest in the exploration of fundamental physics and in the creation of applications [3–8]. In particular, parity-time–($\mathcal{PT}$-) symmetric optical systems proposed with effective magnetic flux allow nonreciprocal light transport [9,10].

$\mathcal{PT}$ symmetry has attracted tremendous interest over the last decade. A $\mathcal{PT}$-symmetric system may possess an entirely real spectrum even though it is non-Hermitian [11–14]. The $\mathcal{PT}$-symmetric system is invariant under the combined parity ($\mathcal{P}$) and time-reversal ($\mathcal{T}$) operators, and its potential fulfills $V^*(x) = V(-x)$. In 2007, a coupled optical waveguide system with an engineered refractive index and gain or loss profile was proposed to realize a $\mathcal{PT}$-symmetric structure [15]. The proposal was based on a classical analogy, namely, that Maxwell's equations describing light propagation under a paraxial approximation are formally equal to a Schrödinger equation [16]. Thereafter, a number of intriguing phenomena could be predicted and experimentally verified, either in a passive or in an active $\mathcal{PT}$-symmetric optical structure, including $\mathcal{PT}$-symmetry breaking [17], power oscillation [18], coherent perfect absorbers [19,20], spectral singularities [21], unidirectional invisibility [22], and nonreciprocal wave propagation [23]. Recently, an active $\mathcal{PT}$-symmetric optical system was realized using two coupled microcavities [24], and optical gain played a key role. Optical isolators [24–26] and $\mathcal{PT}$-symmetric lasers [27–30] were demonstrated; the

gain induced a large optical nonlinearity. Both the coupled optical waveguides and microcavities were described by a tight-binding model. The tight-binding model demonstrated analytical and numerical tractability for study of the $\mathcal{PT}$ symmetry [31–36]. The $\mathcal{PT}$-symmetric phase diagram as well as the wave-packet dynamics in $\mathcal{PT}$-symmetric systems with open boundary conditions have been investigated [37–40]. Although the properties of a lattice with open boundary conditions and the properties of a lattice with periodical boundary conditions are similar as large systems approach a size limit, the differences are notable when the system size is small [41]. Currently, most experimentally accessible $\mathcal{PT}$-symmetric systems are small in size [18,24,26]; hence, studying $\mathcal{PT}$-symmetric systems under periodical boundary conditions is worthwhile, and some pioneering works have already focused on this [41–44].

In this paper, we study the influence of magnetic flux on the $\mathcal{PT}$ symmetry in coupled resonators in a ring configuration [Fig. 1(a)]. The system is modeled by a magnetic tight-binding lattice, with a Peierls phase factor in the hopping between adjacent sites. The one-dimensional ring system has a single pair of balanced gain and loss located at opposite positions; when threaded by magnetic flux, the ring system remains $\mathcal{PT}$ symmetric. We reveal that the $\mathcal{PT}$ symmetry is sensitive to the enclosed magnetic flux, especially when the gain or loss or the system size is large. We find a threshold for the gain or loss above which any nontrivial magnetic flux breaks the $\mathcal{PT}$ symmetry. We also enumerate the eigenvalues that have broken $\mathcal{PT}$ symmetry. The threshold gain or loss as well as the $\mathcal{PT}$-symmetry breaking levels are tunable by the magnetic flux. We present a $\mathcal{PT}$-symmetric phase diagram in the gain and loss and magnetic-flux parameter spaces. The maximally tolerable magnetic flux for the exact $\mathcal{PT}$-symmetric phase is found for a $2N$-site ring system. Our findings offer insights into magnetic flux in $\mathcal{PT}$-symmetric systems and might provide useful applications of $\mathcal{PT}$ symmetry in quantum metrology.

This paper is organized as follows. We formulate a $\mathcal{PT}$-symmetric Hamiltonian threaded by a magnetic flux in Sec. II. We show the energy spectrum and phase diagram of a four-site ring system in Sec. III. We elucidate in detail that the $\mathcal{PT}$ symmetry is significantly affected by the enclosed magnetic flux by studying a $2N$-site ring system in Sec. IV. Our conclusions are drawn in Sec. V.

---
[*]jinliang@nankai.edu.cn

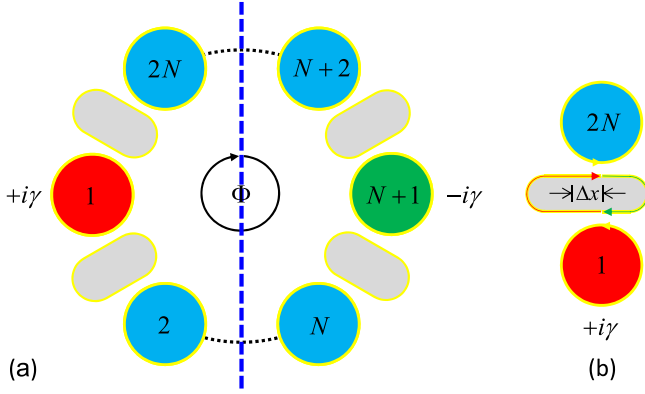FIG. 1. (a) Schematic illustration of a $\mathcal{PT}$-symmetric lattice model using coupled resonators threaded by a magnetic flux Φ. (b) Effective magnetic flux Φ is introduced between resonator 1 and $2N$ through an antiresonant auxiliary resonator (grey). The forward- (green arrow) and backward-going (red arrow) path-length difference Δx induces a nonreciprocal hopping phase $e^{\pm i2\pi\Delta x/\lambda}$.

II. MODEL AND FORMALISM

We consider a discrete $\mathcal{PT}$-symmetric ring system threaded by a magnetic flux. The system is schematically illustrated in Fig. 1(a) using coupled resonators, which constitute a $2N$-site lattice system described by a tight-binding model. The enclosed magnetic flux in the ring system is denoted as Φ. The magnetic flux acts globally: circling photons or charged particles accumulate a phase factor $e^{\pm i\Phi}$ in each round because of the AB effect. The plus (minus) sign represents a clockwise (counterclockwise) direction of motion. The magnetic flux affects the system periodically; the period is 2π, which corresponds to one quantum of the effective magnetic flux. A balanced pair of gain and loss is symmetrically located at opposite positions on sites 1 and $N+1$, respectively. The Hamiltonian for this $2N$-site ring system is given by

$$H_{\text{flux}} = -\sum_{j=1}^{2N}(e^{i\phi}a_j^\dagger a_{j+1} + \text{H.c.}) + i\gamma(a_1^\dagger a_1 - a_{N+1}^\dagger a_{N+1}),$$
(1)

where $a_j^\dagger$ (a_j) is the creation (annihilation) operator for site j, the periodic boundary condition requires $a_{2N+j}^\dagger = a_j^\dagger$. The hopping strength between adjacent sites is set to unity without loss of generality. The balanced gain and loss are conjugate imaginary potentials on sites 1 and $N+1$, the rate is γ ($\gamma > 0$). The enclosed magnetic field effectively induces an additional phase factor $e^{\pm i\phi}$ in the hoppings [Fig. 1(b)], where $\phi = \Phi/(2N)$ is an averaged additional phase between adjacent sites.

The parity operator $\mathcal{P}$ is defined as $\mathcal{P}j\mathcal{P}^{-1} \to N+2-j$, the time-reversal operator $\mathcal{T}$ is defined as $\mathcal{T}i\mathcal{T}^{-1} \to -i$. We note that in the presence of a nontrivial phase factor ($e^{i\Phi} \neq 1$), the system Hamiltonian H_{flux} remains invariant under the combined $\mathcal{PT}$ operator, i.e., $(\mathcal{PT})H_{\text{flux}}(\mathcal{PT})^{-1} = H_{\text{flux}}$. The ring system is $\mathcal{PT}$ symmetric with respect to its central axis [dashed blue line shown in Fig. 1(a)]. When H_{flux} is in its exact $\mathcal{PT}$-symmetric phase, its spectrum is entirely real and all eigenstates are $\mathcal{PT}$ symmetric. When H_{flux} is in its broken

$\mathcal{PT}$-symmetric phase, complex-conjugate pairs emerge and corresponding eigenstates are no longer $\mathcal{PT}$ symmetric. In the following, we discuss how the exact $\mathcal{PT}$-symmetric phase is affected by the parameters of the ring system, in particular, the enclosed magnetic flux and gain or loss.

III. ENERGY SPECTRUM AND PHASE DIAGRAM OF A FOUR-SITE RING SYSTEM

We first consider the simplest case: A four-site $\mathcal{PT}$-symmetric ring system with $N=2$. The Hamiltonian for a four-site ring system is written in the form

$$H_{\text{flux}}^{[4]} = -\sum_{i=1}^{4}(e^{i\phi}a_i^\dagger a_{i+1} + \text{H.c.}) + i\gamma(a_1^\dagger a_1 - a_3^\dagger a_3), \quad (2)$$

where the periodical boundary condition requires $a_{j+4}^\dagger = a_j^\dagger$. The phase factor $e^{\pm i\phi}$ in front of the hoppings between adjacent sites indicates that the enclosed magnetic flux in the ring system is equal to $\Phi = 4\phi$. We can diagonalize the 4×4 matrix to acquire the spectrum of the ring system. The eigenvalue E satisfies $E^2(4 - E^2 - \gamma^2) = 4\sin^2(\Phi/2)$. Solving the equation, we obtain four eigenvalues

$$E = \pm\sqrt{2}\sqrt{\left(1 - \frac{\gamma^2}{4}\right) \pm \sqrt{\left(1 - \frac{\gamma^2}{4}\right)^2 - \sin^2\left(\frac{\Phi}{2}\right)}}. \quad (3)$$

For nontrivial magnetic flux $\Phi \neq 2m\pi$ ($m \in \mathbb{Z}$) changes, the system spectrum changes as the magnetic flux Φ. At $\gamma = 0$, the energy levels shift and form two pairs of doubly degenerate states with energy $E = \pm\sqrt{2}$ when $\Phi = 2m\pi + \pi$ ($m \in \mathbb{Z}$), where the $\mathcal{PT}$ symmetry of the eigenstates is extremely sensitive to the balanced gain and loss, i.e., any nonzero gain or loss ($\gamma \neq 0$) breaks the $\mathcal{PT}$ symmetry.

In the general case, a magnetic flux Φ breaks the $\mathcal{PT}$ symmetry of the eigenstates in the situation that $\cos\Phi < 1 - 2(1 - \gamma^2/4)^2$. The $\mathcal{PT}$-symmetric phase diagram of a four-site ring system is shown in Fig. 2. Region I represents the exact $\mathcal{PT}$-symmetric phase, regions II and III comprise the broken $\mathcal{PT}$-symmetric phase.

The magnetic flux Φ plays different roles as the system gain or loss γ varies in regions of different parameters. For $\gamma = 0$, the dispersion relation is $E = -2\cos(k + \Phi/4)$ with eigenvector $k = 0, \pi/2, \pi, 3\pi/2$. In this case, the magnetic flux Φ shifts the energy spectrum with eigenstates unchanged.

Region I: As γ increases, the ring system is in its exact $\mathcal{PT}$-symmetric phase when $\cos\Phi \geqslant 1 - 2(1 - \gamma^2/4)^2$ in $0 < \gamma < 2$. Region II: The $\mathcal{PT}$ symmetry is broken when $\cos\Phi < 1 - 2(1 - \gamma^2/4)^2$, eigenvalues that are complex-conjugate pairs appear, and the magnetic flux Φ changes both the energy (real part of eigenvalues) and the amplification or decay (imaginary part of the eigenvalues) of the eigenstates. In this case, the region with eigenvalues that are complex-conjugate pairs expands in $0 < \gamma < 2$ but shrinks in $\gamma > 2$ as γ increases. Region III: The magnetic flux Φ changes only the amplification or decay of the eigenstates when $\cos\Phi \geqslant 1 - 2(1 - \gamma^2/4)^2$ in $\gamma \geqslant 2$. This is because the eigenvalues are purely imaginary conjugate pairs in this situation.
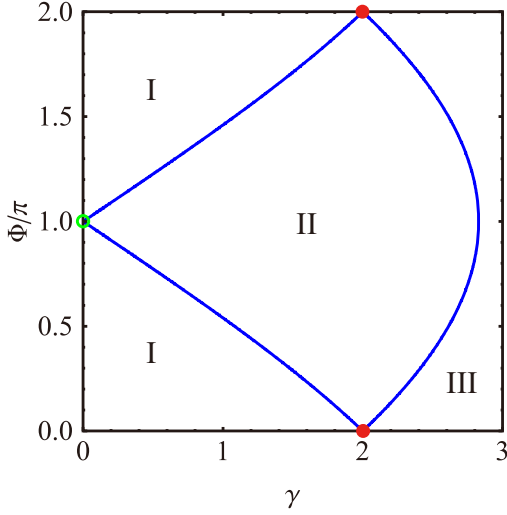
FIG. 2. Phase diagram of a four-site ring system in the parameter spaces γ and Φ. Eigenvalues in region I: Real; region II: Complex conjugate pairs; and region III: Pure imaginary conjugate pairs. Region I is the exact $\mathcal{PT}$-symmetric phase. Region II and III compose the broken $\mathcal{PT}$-symmetric phase. The boundaries (blue curves) indicate the exceptional points where two eigenstates coalescence occurs. The red dots represent the coalescence of three eigenstates, and the green circle represents a Hermitian system without coalescence of eigenstates.

In the trivial magnetic flux $\Phi = 2m\pi$ ($m \in \mathbb{Z}$) case, one complex-conjugate pair becomes a two-fold degenerate state with an eigenvalue of zero in $\gamma > 2$; three energy levels coalesce at $\gamma = 2$ (red dots) with an eigenvalue of zero, and the $\mathcal{PT}$-symmetric ring system becomes a nondiagonalizable Hamiltonian including a 3×3 Jordan block. Figure 2 shows the situation in which nontrivial magnetic flux satisfies $\cos \Phi = 1 - 2(1 - \gamma^2/4)^2$ (excluding the green circle and red dots, e.g., $\gamma = 2\sqrt{2}$, $\Phi = \pi$); this is shown in Fig. 2 by the blue curves that serve as the boundaries of different phases. In this case, two energy levels coalesce, and the $\mathcal{PT}$-symmetric ring system is a nondiagonalizable Hamiltonian composed of two 2×2 Jordan blocks.

IV. EFFECTS OF MAGNETIC FLUX IN THE $\mathcal{PT}$-SYMMETRIC $2N$-SITE RING SYSTEM

The magnetic flux is gauge invariant and acts globally in the ring system. Taking the local transformation $a_j^\dagger \rightarrow e^{i\phi j} a_j^\dagger$, the magnetic flux is unchanged and the Hamiltonian H_{flux} changes into H_{sc} with a nonreciprocal coupling between sites 1 and $2N$. The Hamiltonian H_{sc} is given by

$$H_{\mathrm{sc}} = -\sum_{i=1}^{2N-1}(a_i^\dagger a_{i+1} + \mathrm{H.c.}) - e^{-i\Phi}a_1^\dagger a_{2N} - e^{i\Phi}a_{2N}^\dagger a_1$$
$$+ i\gamma(a_1^\dagger a_1 - a_{N+1}^\dagger a_{N+1}), \qquad (4)$$

which can be realized in coupled optical resonators by introducing synthetic magnetic flux, and a balanced gain and loss in the resonators. The synthetic magnetic flux is introduced through an optical path imbalance method in the coupling process [45]. Consider a system with $2N$ coupled resonators

in a ring configuration. The coupling between resonators 1 and $2N$ is an effective coupling induced by another auxiliary resonator [Fig. 1(b)]. The nonreciprocal phase factor $e^{\pm i\Phi}$ in the hopping between resonators 1 and $2N$ is caused by the optical-path-length difference Δx, which is the difference between the forward-going and backward-going optical paths of the auxiliary resonator in the coupling process. The effective magnetic flux introduced is equal to $\Phi = 2\pi\Delta x/\lambda$ where λ is the optical wavelength [45]. Therefore, Φ is proportional to the path-length difference Δx, and is tunable by changing the position of the auxiliary resonator.

The eigenvalues of the $\mathcal{PT}$-symmetric ring system H_{sc} is calculated as follows. We denote the wave function for eigenvalue E_k as $f_k(j)$. The wave function $f_k(j)$ is assumed as a superposition of forward- and backward-going waves,

$$f_k(j) = \begin{cases} A_k e^{ikj} + B_k e^{-ikj} & (1 \leqslant j \leqslant N+1), \\ C_k e^{ikj} + D_k e^{-ikj} & (N+1 \leqslant j \leqslant 2N). \end{cases} \qquad (5)$$

The Schrödinger equation for site j in the ring system (excluding sites 1, $N+1$, and $2N$) is given as

$$f_k(j-1) + f_k(j+1) + E_k f_k(j) = 0, \qquad (6)$$

and substituting the wave functions of Eq. (5) into Eq. (6), we obtain the eigenvalue $E_k = -2\cos k$.

The Schrödinger equations for sites 1, $N+1$, and $2N$ are

$$f_k(2) + e^{-i\Phi}f_k(2N) - (i\gamma - E_k)f_k(1) = 0, \qquad (7)$$

$$e^{i\Phi}f_k(1) + f_k(2N-1) + E_k f_k(2N) = 0, \qquad (8)$$

$$f_k(N+2) + f_k(N) + (i\gamma + E_k)f_k(N+1) = 0. \qquad (9)$$

From the continuity of the wave function on site $N+1$, the wave function $f_k(N+1)$ should satisfy

$$A_k e^{i(N+1)k} + B_k e^{-i(N+1)k} = C_k e^{i(N+1)k} + D_k e^{-i(N+1)k}, \qquad (10)$$

After simplification of the Schrödinger equations and the continuity equation shown in Eqs. (7)–(10), we derive a critical equation for eigenvector k as an implicit function of the gain/ or loss γ and the enclosed magnetic flux Φ. The critical equation for eigenvector k has the form

$$\left(1 - \frac{\gamma^2}{4\sin^2 k}\right)\sin^2(Nk) - \sin^2\left(\frac{\Phi}{2}\right) = 0. \qquad (11)$$

In the situation of a trivial magnetic flux $\Phi = 2m\pi$ ($m \in \mathbb{Z}$), the gain or loss affects only one pair of energy levels; it leaves the others unchanged. The spectrum of a $2N$-site ring system includes $N-1$ pairs of two-fold degenerate energy levels, i.e., $-2\cos(n\pi/N)$ with $n \in [1, N-1]$ (indicated by blue lines in Fig. 3); and one pair of gain- or loss-dependent energy levels, i.e., $\pm\sqrt{4 - \gamma^2}$ (indicated by dashed red lines in Fig. 3). When the gain or loss $\gamma > 2$, the ring system is in its broken $\mathcal{PT}$-symmetric phase, and the system spectrum has one conjugate pair.

To analyze the influence of magnetic flux on the system spectrum, we denote the left side of the critical equation Eq. (11) as $\mathcal{F}(\gamma, \Phi, k)$, which is a function of parameters γ, Φ for eigenvector $k \neq 0$ (note that $k = 0$ is not the eigenvector

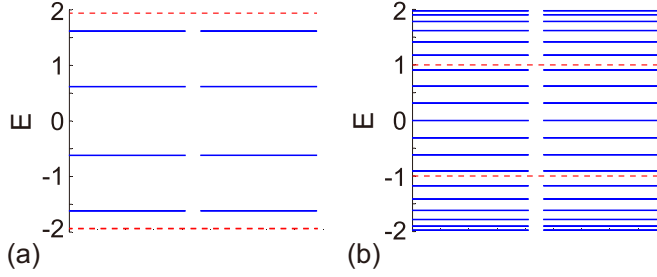FIG. 3. Energy levels for a ring system under trivial magnetic flux $\Phi = 2m\pi$ ($m \in \mathbb{Z}$) with (a) $N = 5$, $\gamma = 0.5$ and (b) $N = 20$, $\gamma = \sqrt{3}$. The spectrum includes $N - 1$ pairs of two-fold degenerate energy levels $-2\cos(n\pi/N)$ where $n \in [1, N - 1]$ (solid blue lines), and also two γ-dependent energy levels $\pm\sqrt{4 - \gamma^2}$ (dashed red lines).

when $\gamma \neq 0$),

$$\mathcal{F}(\gamma, \Phi, k) = \left(1 - \frac{\gamma^2}{4\sin^2 k}\right)\sin^2(Nk) - \sin^2\left(\frac{\Phi}{2}\right). \quad (12)$$

The real eigenvector k with $\mathcal{F}(\gamma, \Phi, k) = 0$ corresponds to the real eigenvalue E_k of the $\mathcal{PT}$-symmetric $2N$-site ring system. For a situation with gain or loss $\gamma > 2$, we have $\mathcal{F}(\gamma, \Phi, k) < 0$ for any nontrivial magnetic flux $\Phi \neq 2m\pi$ ($m \in \mathbb{Z}$); this indicates that the spectrum of the ring system is entirely constituted by conjugate pairs without any real eigenenergy. For magnetic flux $\Phi = 2m\pi + \pi$ ($m \in \mathbb{Z}$), we have $\mathcal{F}(\gamma, \Phi, k) = -\cos^2(Nk) - \gamma^2\sin^2(Nk)/(4\sin^2 k) < 0$, and the real eigenvector k is absent, i.e., the system spectrum is entirely constituted by conjugate pairs at $\gamma \neq 0$.

The $\mathcal{PT}$-symmetric $2N$-site ring system has at most one conjugate pair in its spectrum when the magnetic flux is $\Phi = 2m\pi$ ($m \in \mathbb{Z}$), but it has at most N conjugate pairs when $\Phi = 2m\pi + \pi$ ($m \in \mathbb{Z}$). This implies the system spectrum is sensitive to magnetic flux, and the number of conjugate pairs appreciably varies with the magnetic flux. In the following, we systemically investigate how $\mathcal{PT}$ symmetry of the eigenstates is affected by the magnetic flux and gain or loss. We first consider a trivial case of effective magnetic flux with $\Phi = 2m\pi$ ($m \in \mathbb{Z}$): the function $\mathcal{F}(\gamma, \Phi, k)$ reduces to $\mathcal{F}(\gamma, \Phi, k) = [1 - \gamma^2/(4\sin^2 k)]\sin^2(Nk)$. $\mathcal{F}(\gamma, \Phi, k) = 0$ is the critical equation for the eigenvector k. We find the eigenvalues are $-2\cos(n\pi/N)$ with $n \in [1, N - 1]$ and $\pm\sqrt{4 - \gamma^2}$. The gain or loss γ only changes two energy levels, $\epsilon_\pm = \mp\sqrt{4 - \gamma^2}$, the eigenvector for ϵ_+ is

$$k_+ = \arccos\sqrt{1 - \gamma^2/4}. \quad (13)$$

Hence, when $k_+ < \pi/N$, the system spectrum may be entirely real even if $\Phi \neq 2m\pi$ ($m \in \mathbb{Z}$). This indicates a threshold gain or loss value, $\gamma_c = 2\sin(\pi/N)$. When the gain/or loss is below the threshold ($\gamma < \gamma_c$), the ring system can be in an exact $\mathcal{PT}$-symmetric phase. As magnetic flux increases from 0 to π, the energy levels with broken $\mathcal{PT}$ symmetry simultaneously emerge from 1 to N pairs. If $\gamma > \gamma_c$, the $\mathcal{PT}$ symmetry is extremely sensitive to the magnetic flux; any nontrivial magnetic flux $\Phi \neq 2m\pi$ ($m \in \mathbb{Z}$) breaks the $\mathcal{PT}$ symmetry and causes conjugate pairs to emerge simultaneously. Above the threshold gain or loss ($\gamma > \gamma_c$), the ring system remains in an exact $\mathcal{PT}$-symmetric phase only when $\Phi = 2m\pi$ ($m \in \mathbb{Z}$).
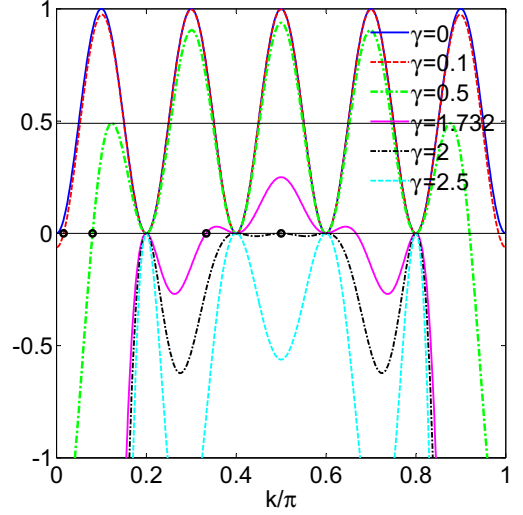

FIG. 4. $\mathcal{F}(\gamma, 0, k)$ for a ring system with $N = 5$ at various gains or losses: $\gamma = 0$ (solid blue), 0.1 (dashed red), 0.5 (dash-dotted green), $\sqrt{3}$ (solid magenta), 2 (dash-dotted black), and 2.5 (dashed cyan). The black circles show $k_+ = \arccos(\sqrt{1 - \gamma^2/4})$ for $\gamma = 0.1$, 0.5, $\sqrt{3}$, 2. In the region $\gamma > 2$ (e.g., $\gamma = 2.5$), no real k_+ exists, any $\Phi \neq 2m\pi$ ($m \in \mathbb{Z}$) brings all $2N$ eigenvalues into conjugate pairs. The horizontal black lines are guides to the eye, which indicate $\sin^2(\Phi/2)$ for a trivial magnetic flux and the maximal magnetic flux that allows exact $\mathcal{PT}$ symmetry at $\gamma = 0.5$.

Moreover, the minimal number of complex eigenvalue pairs in the presence of nontrivial magnetic flux is

$$D = 2[k_+ N/\pi], \quad (14)$$

where $[x]$ stands for the integer part of x.

As shown in Fig. 3(a), when $\gamma = 0.5 < \gamma_c = 2\sin(\pi/5)$, the ring system keeps in the exact $\mathcal{PT}$-symmetric phase in the presence of nontrivial magnetic flux. In Fig. 3(b), $\gamma = \sqrt{3} > \gamma_c = 2\sin(\pi/20)$ and $k_+ = \pi/3$; the minimal number of energy levels with broken $\mathcal{PT}$ symmetry is $D = 12$ for nontrivial magnetic flux; the nontrivial magnetic flux breaks the $\mathcal{PT}$ symmetry of the energy levels with $|E_k| > \sqrt{4 - \gamma^2}$.

We plot function $\mathcal{F}(\gamma, 0, k)$ for a ring system with $N = 5$ in Fig. 4. We can see how the eigenvector is changed into a complex number by the variations of γ and Φ. In Fig. 4, $\mathcal{F}(\gamma, 0, k)$ for the ring system at $\gamma = 0$, 0.1, 0.5, $\sqrt{3}$, 2, 2.5 are plotted. The black circles stand for the eigenvector $k_+ = \arccos(\sqrt{1 - \gamma^2/4})$ for $\gamma = 0.1$, 0.5, $\sqrt{3}$, 2. Note that all $2N$ eigenvalues become conjugate pairs for nontrivial magnetic flux when $\gamma \geqslant 2$, and for nonzero gain or loss when $\Phi = 2m\pi + \pi$ ($m \in \mathbb{Z}$).

Figure 5 shows the energy bands found by numerical diagonalization of H_{sc} in Eq. (4) with $N = 5$; the corresponding eigenvector k is in accord with the eigenvector from the critical equation Eq. (11). For trivial magnetic flux, the $\mathcal{PT}$-symmetric ring system has only one complex pair when $\gamma > 2$. For nontrivial flux, the energy level degeneracy (Fig. 3) disappears. This is because the nonreciprocal hopping between the coupled resonators breaks the time-reversal symmetry in the tunneling. The number of conjugate pairs changes from 1 (D) to N as magnetic flux Φ increases from 0 to π for gain or loss below
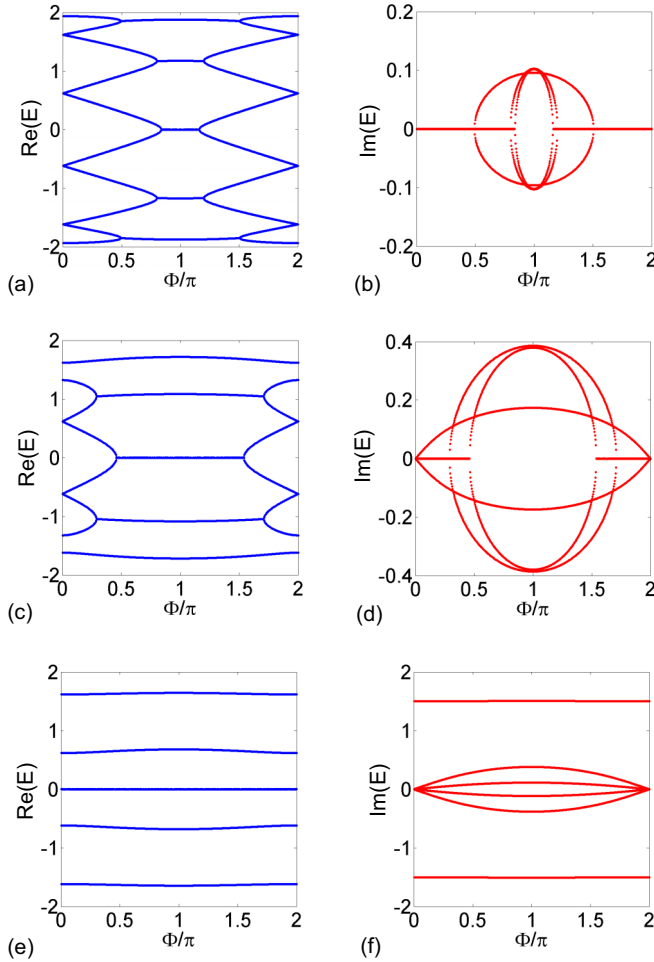
FIG. 5. Energy band of a ring system with $N = 5$ at various gain and loss values. (a),(b) $\gamma = 0.5$, (c),(d) $\gamma = 1.5$, and (e),(f) $\gamma = 2.5$. The real parts (in blue) and imaginary parts (in red) are in the left and right panels, respectively.

(above) the threshold. Figure 5 shows the magnetic flux acting globally, and the spectrum structure substantially varies with the magnetic flux at different values of gain or loss.

Now we focus on the influence of magnetic flux on the $\mathcal{PT}$-symmetric phase diagram. To get the $\mathcal{PT}$-symmetric phase diagram, we define Φ_c as the maximal magnetic flux that keeps a ring system in its exact $\mathcal{PT}$-symmetric phase. The maximal magnetic flux Φ_c depends on the non-Hermitian γ and indicates the boundary of the $\mathcal{PT}$-symmetric phase diagram in the Φ and γ parameter spaces. For a gain or loss above the threshold, $\gamma > \gamma_c = 2\sin(\pi/5) \approx 1.1756$, any nontrivial magnetic flux $\Phi \neq 2m\pi$ ($m \in \mathbb{Z}$) breaks the $\mathcal{PT}$ symmetry. In this situation, Φ_c is zero. The $\mathcal{PT}$ symmetry is extremely sensitive to magnetic flux for large values of γ or N (the gain or loss threshold γ_c depends on N).

For a gain or loss below the threshold, $\gamma < \gamma_c = 2\sin(\pi/5) \approx 1.1756$, e.g., $\gamma = 0.5$ (Fig. 4, indicated by the dash-dotted green line), the $\mathcal{PT}$ symmetry is robust to the magnetic flux Φ when $\sin^2(\Phi/2)$ is in the region between the two horizontal black lines shown in Fig. 4. In this situation, the magnetic flux does not break $\mathcal{PT}$ symmetry, and the system spectrum is entirely real. If γ or Φ increases from
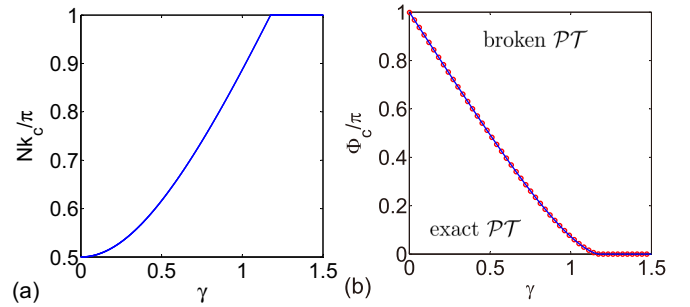

FIG. 6. (a) Numerically determined k_c where $\mathcal{F}(\gamma, 0, k)$ is at its maximum in region $[\pi/2N, \pi/N]$. (b) Numerically determined maximum magnetic flux Φ_c as a function of γ. The lower left (upper right) region is the exact (broken) $\mathcal{PT}$-symmetric phase. The ring system is with $N = 5$.

0, the system goes through a $\mathcal{PT}$-symmetric breaking phase transmission when $\mathcal{F}(\gamma, 0, k) < \sin^2(\Phi/2)$ for $k \in [0, \pi/N]$. Then the entirely real spectrum disappears and conjugate pairs emerge. For each γ, the ring system is in its exact $\mathcal{PT}$-symmetric phase when the magnetic flux is below the maximal value Φ_c.

To gain insight into $\mathcal{PT}$ symmetry under magnetic flux, we set the function $\mathcal{F}(\gamma, 0, k)$ to reach its maximum at k_c in the region $k \in [0, \pi/N]$, where k_c can be calculated from $d\mathcal{F}(\gamma, 0, k)/dk = 0$. We plot k_c and Φ_c in Fig. 6; the blue lines are obtained by numerically solving the equation $d\mathcal{F}(\gamma, 0, k)/dk = 0$. The red circles are obtained by numerically diagonalizing the ring system Hamiltonian; the results from these two methods are in accord with each other. In Fig. 6(a), we plot Nk_c as a function of γ for the ring system with $N = 5$. As γ increases from 0 to γ_c, k_c increases from $\pi/(2N)$ to π/N, the maximal value of $\mathcal{F}(\gamma, 0, k_c)$ decreases from 1 to 0, and the maximum magnetic flux Φ_c decreases from π to 0 [Fig. 6(b)]. Figure 6(b) shows the $\mathcal{PT}$-symmetry phase diagram of the ring system. We can see the sharp changes at $Nk_c = \pi$ in Fig. 6(a), and $\Phi_c = 0$ at $\gamma_c \approx 1.1756$ in Fig. 6(b).

The maximal magnetic flux Φ_c keeps the ring system in the exact $\mathcal{PT}$-symmetric phase; it satisfies $\mathcal{F}(\gamma, \Phi_c, k_c) = 0$. We numerically calculate the maximum magnetic flux Φ_c, which increases as the gain or loss γ decreases. The maximal magnetic flux Φ_c as a function of γ is shown in Fig. 7; the colored lines and markers are numerical results from the theoretical analysis and exact diagonalization of H_{sc}, respectively. For weak γ ($\gamma \lesssim \pi/N$), we approximately have $k_c \approx \pi/(2N)$. Correspondingly, the maximal magnetic flux is approximately linearly dependent on γ as $\Phi_c/\pi \approx 1 - (2N/\pi^2)\gamma$ (indicated by dashed black lines in Fig. 7). The maximum magnetic flux Φ_c decreases as ring system size N increases.

The $\mathcal{PT}$-symmetric phase transition is closely related to the magnetic flux in the coupled resonators enclosed magnetic flux. By tuning the coupling position of the auxiliary resonator between resonators 1 and $2N$ [Fig. 1(b)], the path lengths of forward- and backward-going directions change, which linearly affects the magnetic flux. The $\mathcal{PT}$-symmetry breaking point varies with the magnetic flux; the gain or loss threshold for $\mathcal{PT}$-symmetry breaking can be greatly reduced by increasing the enclosed magnetic flux from zero to half a
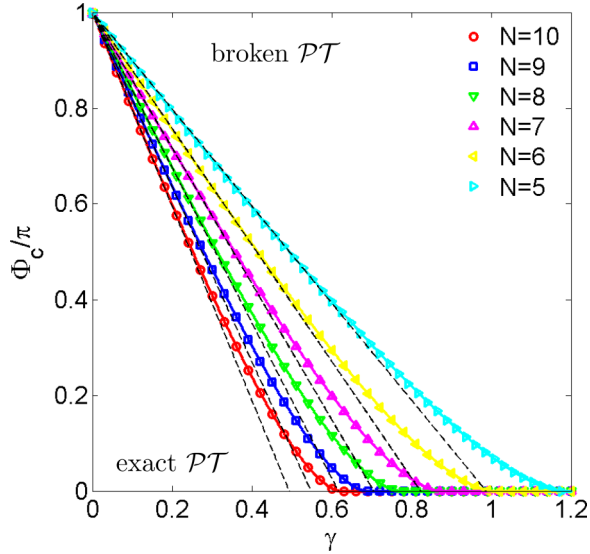
FIG. 7. Maximum magnetic flux Φ_c as a function of γ for a ring system with $N = 5$ to 10. The colored lines (markers) are the numerically obtained theoretical analysis (exact diagonalization) of the Hamiltonian H_{sc}. The dashed black lines indicate $\Phi_c/\pi \approx 1 - (2N/\pi^2)\gamma$.

V. CONCLUSIONS

We investigate $\mathcal{PT}$-symmetric non-Hermitian coupled resonators in ring configurations threaded by an effective magnetic flux. The ring system is described by a $2N$-site tight-binding model; the ring system has a balanced pair of gain and loss located at two opposite sites. We demonstrate that the system's $\mathcal{PT}$ symmetry is extremely sensitive to the enclosed magnetic flux when the gain or loss is above a threshold $\gamma_c = 2\sin(\pi/N)$. We find the minimal number of conjugate pairs emerging in the system spectrum when the $\mathcal{PT}$ symmetry is breaking in the presence of nontrivial magnetic flux. The system eigenvalues all become conjugate pairs at a magnetic flux $\Phi = 2m\pi + \pi$ ($m \in \mathbb{Z}$) for any nonzero γ; or at a gain or loss twice as large as the hopping strength ($\gamma > 2$) for any nontrivial magnetic flux Φ. We show the $\mathcal{PT}$-symmetric phase diagram in the parameter spaces of γ and Φ. The results indicate that the maximal magnetic flux approximately linearly depends on γ as $\Phi_c/\pi \approx 1 - (2N/\pi^2)\gamma$ in the weak γ region ($\gamma \lesssim \pi/N$). The maximal magnetic flux decreases as the gain or loss or the system size increases. Our findings indicate that $\mathcal{PT}$ symmetry is very sensitive to the nonlocal vector potential in this $\mathcal{PT}$-symmetric non-Hermitian system. These results could be useful in quantum metrology in the future.

quantum. The $\mathcal{PT}$-symmetry breaking energy levels change from one pair to N pairs when the enclosed magnetic flux is so tuned. The $\mathcal{PT}$-symmetry breaking can be observed at low balanced gain and loss values in coupled resonators with enclosed magnetic flux.

[1] W. Ehrenberg and R. E. Siday, Proc. Phys. Soc. (London) **B62**, 8 (1949).

[2] Y. Aharonov and D. Bohm, Phys. Rev. **115**, 485 (1959).

[3] K. Fang and S. Fan, Phys. Rev. A **88**, 043847 (2013).

[4] K. Fang, Z. Yu, and S. Fan, Nat. Photon. **6**, 782 (2012).

[5] E. Li, B. J. Eggleton, K. Fang, and S. Fan, Nat. Commun. **5**, 3225 (2014).

[6] M. Hafezi, E. A. Demler, M. D. Lukin, and J. M. Taylor, Nat. Phys. **7**, 907 (2011).

[7] M. Hafezi, S. Mittal, J. Fan, A. Migdall, and J. M. Taylor, Nat. Photon. **7**, 1001 (2013).

[8] G. Q. Liang and Y. D. Chong, Phys. Rev. Lett. **110**, 203904 (2013).

[9] S. Longhi, Opt. Lett. **40**, 1278 (2015).

[10] X. Q. Li, X. Z. Zhang, G. Zhang, and Z. Song, Phys. Rev. A **91**, 032101 (2015).

[11] C. M. Bender and S. Boettcher, Phys. Rev. Lett. **80**, 5243 (1998); C. M. Bender, D. C. Brody, and H. F. Jones, *ibid.* **89**, 270401 (2002).

[12] A. Mostafazadeh, J. Math. Phys. **43**, 205 (2002); **43**, 3944 (2002).

[13] M. Znojil, Phys. Lett. A **259**, 220 (1999); **264**, 108 (1999); **285**, 7 (2001).

[14] P. Dorey, C. Dunning, and R. Tateo, J. Phys. A **34**, 5679 (2001).

[15] R. El-Ganainy, K. G. Makris, D. N. Christodoulides, and Z. H. Musslimani, Opt. Lett. **32**, 2632 (2007).

[16] S. Longhi, Laser Photon. Rev. **3**, 243 (2009).

[17] A. Guo, G. J. Salamo, D. Duchesne, R. Morandotti, M. Volatier-Ravat, V. Aimez, G. A. Siviloglou, and D. N. Christodoulides, Phys. Rev. Lett. **103**, 093902 (2009).

[18] C. E. Rüter, K. G. Makris, R. El-Ganainy, D. N. Christodoulides, M. Segev, and D. Kip, Nat. Phys. **6**, 192 (2010).

[19] Y. D. Chong, L. Ge, H. Cao, and A. D. Stone, Phys. Rev. Lett. **105**, 053901 (2010).

[20] Y. Sun, W. Tan, H. Q. Li, J. Li, and H. Chen, Phys. Rev. Lett. **112**, 143903 (2014).

[21] A. Mostafazadeh, Phys. Rev. Lett. **102**, 220402 (2009); **110**, 260402 (2013).

[22] Z. Lin, H. Ramezani, T. Eichelkraut, T. Kottos, H. Cao, and D. N. Christodoulides, Phys. Rev. Lett. **106**, 213901 (2011).

[23] L. Feng, Y. L. Xu, W. S. Fegadolli, M. H. Lu, J. E. B. Oliveira, V. R. Almeida, Y. F. Chen, and A. Scherer, Nat. Mater. **12**, 108 (2013).

[24] B. Peng, S. K. Özdemir, F. Lei, F. Monifi, M. Gianfreda, G. L. Long, S. Fan, F. Nori, C. M. Bender, and L. Yang, Nat. Phys. **10**, 394 (2014).

[25] B. Peng, S. K. Özdemir, W. Chen, F. Nori, and L. Yang, Nat. Commun. **5**, 5082 (2014).

[26] L. Chang, X. Jiang, S. Hua, C. Yang, J. Wen, L. Jiang, G. Li, G. Wang, and M. Xiao, Nat. Photon. **8**, 524 (2014).

[27] H. Jing, S. K. Özdemir, X.-Y. Lü, J. Zhang, L. Yang, and F. Nori, Phys. Rev. Lett. **113**, 053604 (2014).

[28] B. Peng, S. K. Özdemir, S. Rotter, H. Yilmaz, M. Liertzer, F. Monifi, C. M. Bender, F. Nori, and L. Yang, Science **346**, 328 (2014).

[29] L. Feng, Z. J. Wong, R.-M. Ma, Y. Wang, and X. Zhang, Science **346**, 972 (2014).

[30] H. Hodaei, M.-A. Miri, M. Heinrich, D. N. Christodoulides, and M. Khajavikhan, Science **346**, 975 (2014).

[31] O. Bendix, R. Fleischmann, T. Kottos, and B. Shapiro, Phys. Rev. Lett. **103**, 030402 (2009).

[32] S. Longhi, Phys. Rev. Lett. **103**, 123601 (2009); Phys. Rev. B **80**, 235102 (2009); **81**, 195118 (2010); Phys. Rev. A **82**, 032111 (2010); Phys. Rev. B **82**, 041106(R) (2010).

[33] S. Longhi, J. Phys. A: Math. Theor. **47**, 165302 (2014).

[34] M. Znojil, J. Phys. A: Math. Theor. **41**, 292002 (2008); Phys. Rev. A **82**, 052113 (2010); J. Phys. A: Math. Theor. **44**, 075302 (2011).

[35] M. Znojil, J. Phys. A: Math. Theor. **47**, 435302 (2014); Ann. Phys. (NY) **361**, 226 (2015).

[36] L. Jin and Z. Song, Phys. Rev. A **80**, 052107 (2009); **81**, 032109 (2010).

[37] Y. N. Joglekar, D. Scott, M. Babbey, and A. Saxena, Phys. Rev. A **82**, 030103(R) (2010).

[38] Y. N. Joglekar and A. Saxena, Phys. Rev. A **83**, 050101(R) (2011).

[39] D. D. Scott and Y. N. Joglekar, Phys. Rev. A **83**, 050102(R) (2011).

[40] Y. N. Joglekar, D. D. Scott, and A. Saxena, Phys. Rev. A **90**, 032108 (2014).

[41] D. D. Scott and Y. N. Joglekar, Phys. Rev. A **85**, 062105 (2012).

[42] L. Jin and Z. Song, Phys. Rev. A **84**, 042116 (2011); W. H. Hu, L. Jin, Y. Li, and Z. Song, *ibid.* **86**, 042110 (2012).

[43] H. Vemuri and Y. N. Joglekar, Phys. Rev. A **87**, 044101 (2013).

[44] S. Longhi, Phys. Rev. A **88**, 062112 (2013).

[45] M. Hafezi, Phys. Rev. Lett. **112**, 210405 (2014).